

Status report on C-130 air-motion measurements

July 29, 2005

We report here some problems that we observed in the in situ measurements of air velocity fluctuations on the NCAR C-130 aircraft during DYCOMS-II and the impact of the recent re-processing of the dataset.

The following departures from their expected behaviour were noted on the spectra and the momentum fluxes in the original dataset:

1. The ratios between the transverse spectra and the longitudinal spectrum do not take the expected value of $4/3$ in the inertial subrange;
2. The vertical velocity spectrum follows a -2 slope rather than the predicted $-5/3$ slope in the inertial subrange;
3. The momentum fluxes seem to be biased by a spurious covariance between air vertical velocity and true airspeed, which is manifested in the component of momentum flux along the longitudinal axis of the airplane.

We find that the re-processing (mainly the new static pressure calibration) reduces the momentum flux bias to 25% of its previous value. However, the two other spectral inconsistencies (1. and 2.) remain in the new dataset.

Notation:

u_a : True airspeed (*TASHC*),

u_p : Ground speed (function of *VEWC* and *VNSC*),

u : East component of the wind (*UIC*),

v : North component of the wind (*VIC*),

w : Vertical gust component (*WIC*),

u_x : Longitudinal component (*UXC*),

v_y : Lateral component (*VYC*),

u' : fluctuations of u ,

$\langle u'w' \rangle$: Covariance between u and w , calculated on 30 second segments averaged over 2.5 minutes.

The true heading angle chosen to represent each flux measurement is the true heading angle corresponding to the middle of the time segment.

The spectra calculation was also based on 2.5 minutes segments.

We discuss here the momentum fluxes and spectra calculated for the circles flown during DYCOMS-II for two kinds of datasets. The first is the dataset that was available to the DYCOMS-II community. The second is a re-processed dataset, with mainly a change of the static pressure calibration and a few other changes.

All boundary-layer circle legs of all flights are considered (RF0- 1, 2, 3, 4, 5, 7, 8).

Momentum fluxes

In the first set of figures, East and North components of the momentum fluxes, as well as the longitudinal and transverse components are displayed as a function of the true heading angle.

Calculating the momentum fluxes during DYCOMS-II along each circle of all the 7 flights, we found an unexpected dependence on the true heading angle for $\langle u'w' \rangle$ and $\langle v'w' \rangle$ in the original dataset (see Fig. 1). A real sinusoidal dependence on angle around the circle of a given flight could be possible only if there were a real horizontal gradient of the flux. But the circle flown in the opposite direction should then show the exact opposite sinusoid. From one level to the other and from one flight to the other, the horizontal gradient would also likely have a different direction and would lead to different phase shifts in the sinusoid on different days. Therefore we would not expect to see such a sinusoid when all the legs are combined.

This heading-dependence seems to be due to a spurious covariance between the true air speed and the vertical velocity (Fig. 5, top panel). Since $u_x \approx u_a - u_p$, and since we

do not observe the same covariance between the ground speed and the vertical velocity (Fig. 5 , bottom panel), the covariance between u_a and w is manifested by a bias in $\langle u'_x w' \rangle$ (also seen on Fig. 7).

The equations

$$\langle u' w' \rangle = \langle u'_x w' \rangle \sin \psi - \langle v'_y w' \rangle \cos \psi \quad (1)$$

$$\langle v' w' \rangle = \langle u'_x w' \rangle \cos \psi + \langle v'_y w' \rangle \sin \psi \quad (2)$$

show that any bias in $\langle u'_x w' \rangle$ leads to a spurious sinusoidal signal in $\langle u' w' \rangle$ and $\langle v' w' \rangle$ as function of true heading angle.

A new static pressure calibration has been used in the new dataset. In the original dataset, the calibration is calculated as a linear function of the dynamic pressure. The new calibration is calculated as a linear function of the ratio of the attack angle differential pressure to the dynamic pressure. Other changes were made (to be documented). One among them took care of a leak in the static pressure tube.

The covariance between u_a and w is reduced in this re-processed dataset (Fig. 6); therefore so is the bias of the longitudinal momentum flux $\langle u'_x w' \rangle$ (Fig. 4 and Fig. 8). Consequently, the spurious sinusoidal curve on the East and North component of the momentum fluxes is attenuated in the new dataset (Fig. 2) (to 25% of its previous value).

In the original dataset, we found a significant coherence between true air speed and vertical velocity around 0.3 Hz. Fig. 12 shows that this coherence is now much reduced in this range, but slightly increased at around 3 Hz.

Spectra

Fig. 9 shows that the new calibration attenuates the spectral energy of the longitudinal component in the same range of 0.3 Hz mentioned above, while the spectra of the lateral and vertical components are slightly changed by the new calibration, with more energy around 0.2 Hz. The observation of a steeper (than $-5/3$) slope for the vertical component (Fig. 11) and of a ratio close to 1 between transverse and longitudinal spectra rather than the theoretical $4/3$ (not shown), remain in the new dataset.

Next step

We will look more thoroughly at spectral properties of the vertical velocity, and specifically study the spectra of the input variables from which it is calculated, to try elucidate the reason for the steep slope of its spectrum.

We will also check if the peculiarities of the spectra seen during DYCOMS are also observed during EPIC (with straight legs rather than circle legs) and RICO (as a more recent program).

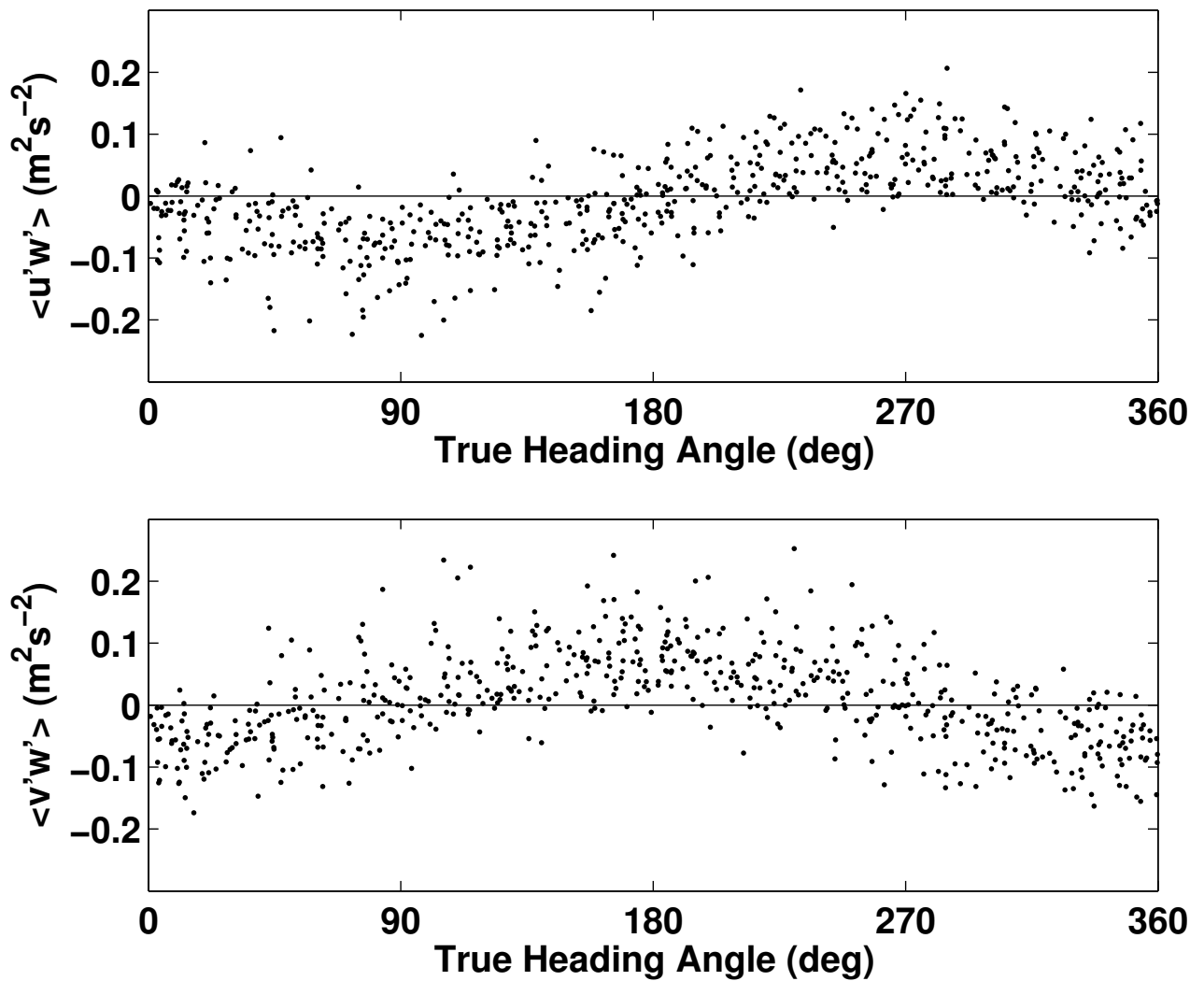


Figure 1: East (top) and North (bottom) components of the vertical momentum flux, as a function of the true heading angle, for all legs and all flights. Original dataset.

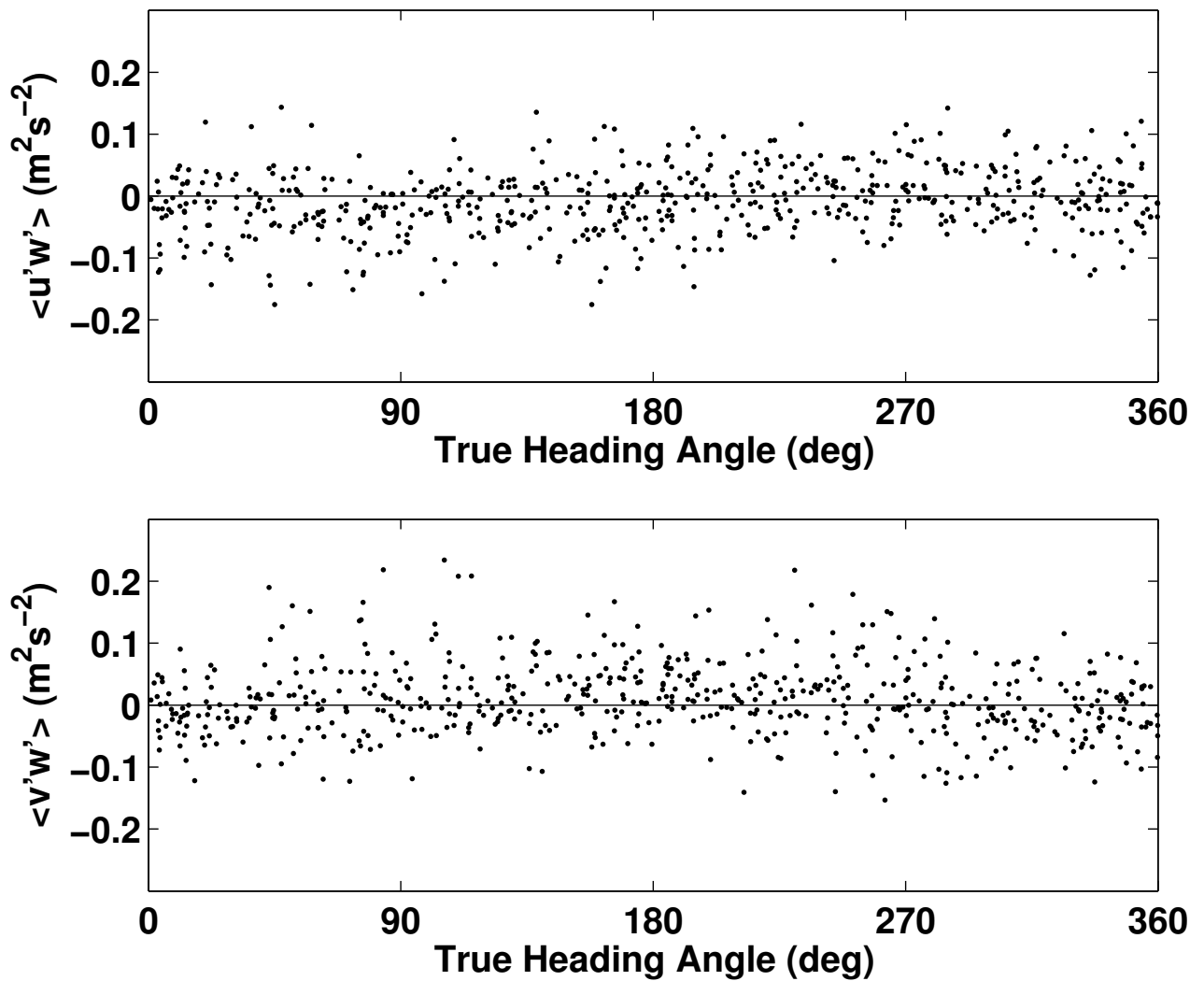


Figure 2: East (top) and North (bottom) component of the vertical momentum flux, as a function of the true heading angle for all legs and all flights. New dataset.

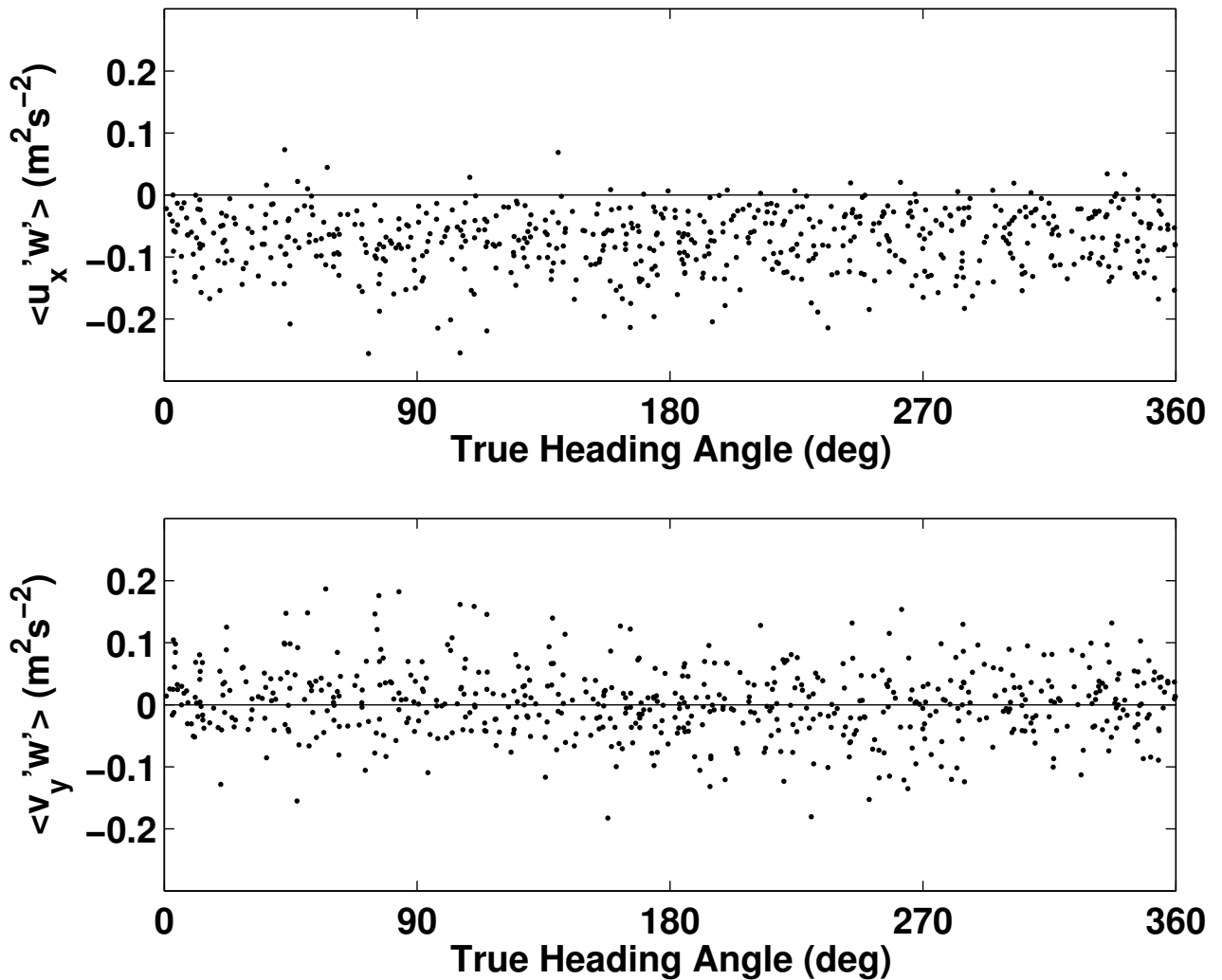


Figure 3: Longitudinal (top) and transverse (bottom) components of the vertical momentum flux, as a function of the true heading angle, for all legs and all flights. Original dataset.

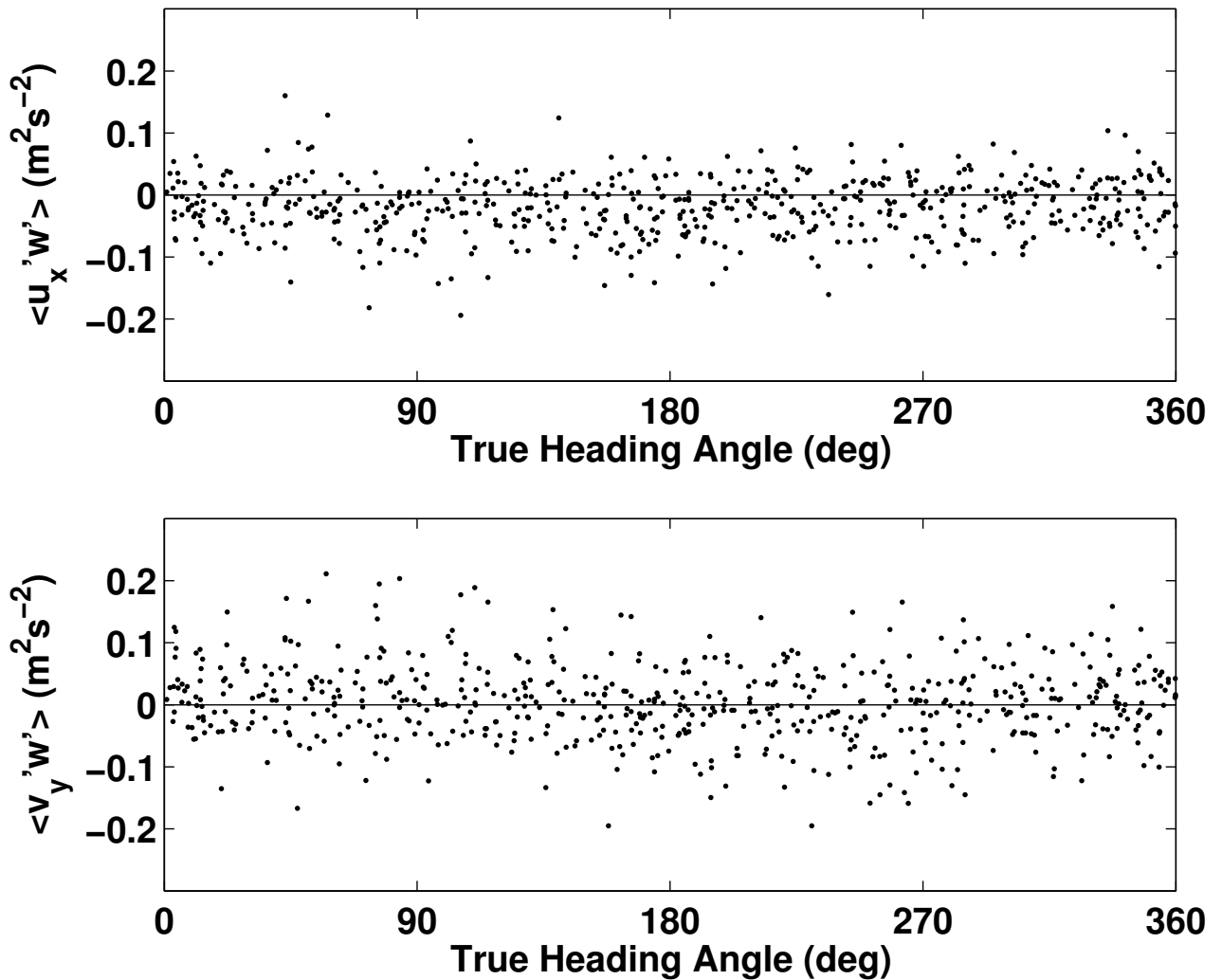


Figure 4: Longitudinal (top) and transverse (bottom) components of the vertical momentum flux, as a function of the true heading angle, for all legs and all flights. New dataset.

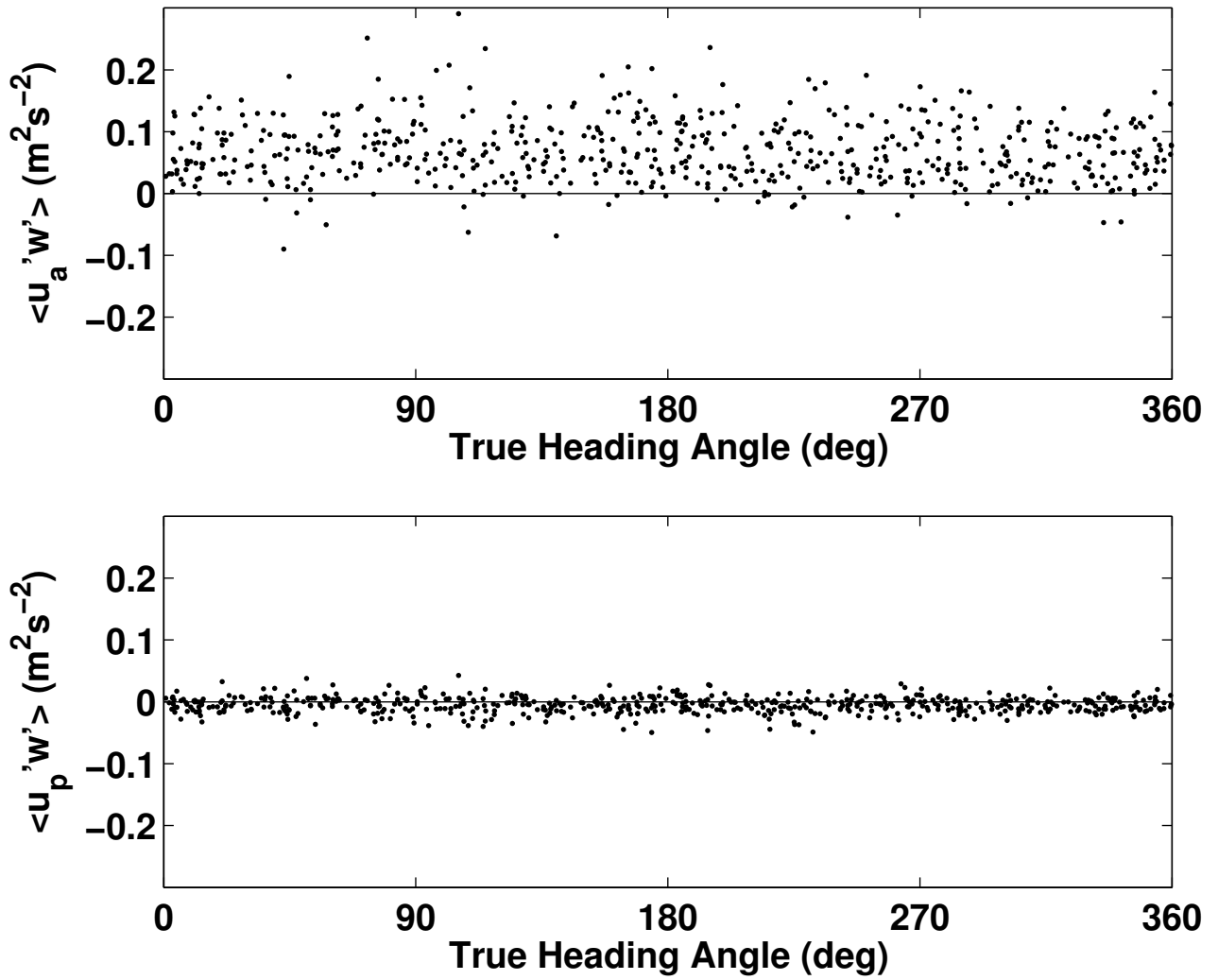


Figure 5: Covariance between the true air speed and the vertical velocity (top) and between the ground speed and the vertical velocity (bottom), as a function of the true heading angle, for all legs and all flights. Original dataset.

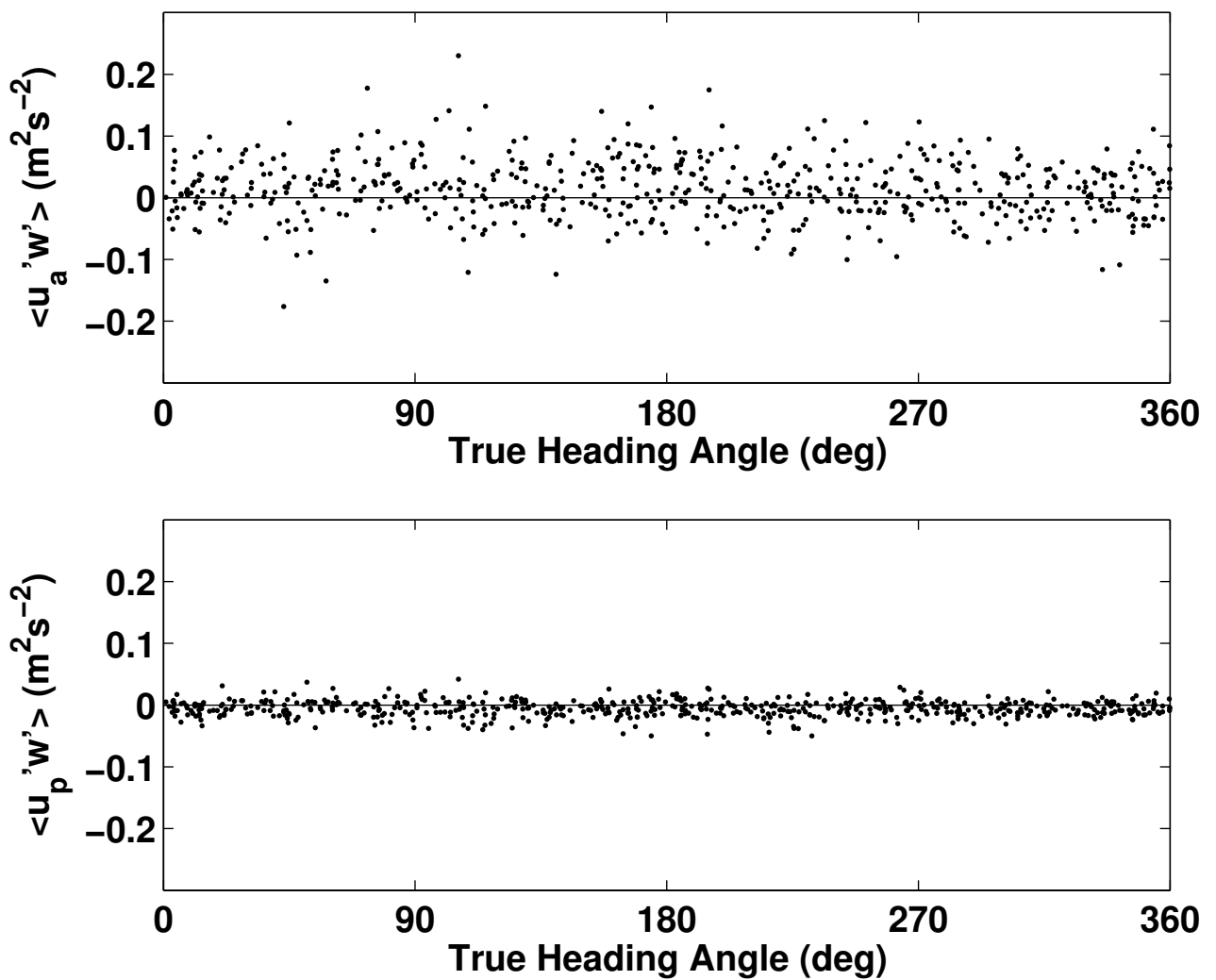


Figure 6: Covariance between the true air speed and the vertical velocity (top) and between the ground speed and the vertical velocity (bottom), as a function of the true heading angle, for all legs and all flights. New dataset.

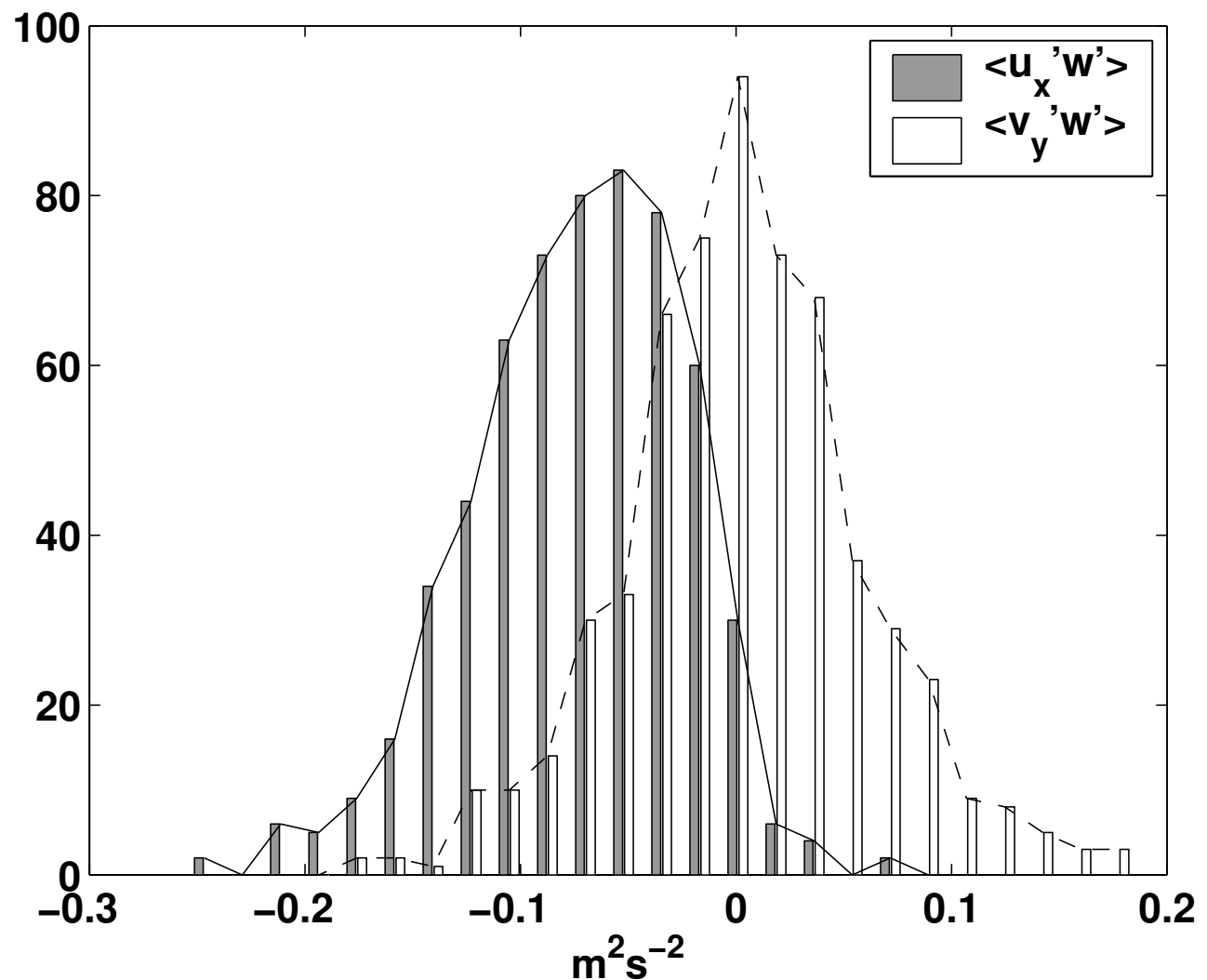


Figure 7: Distributions of the longitudinal (top) and transverse (bottom) components of the momentum flux. All legs and all flights are included. Old dataset.

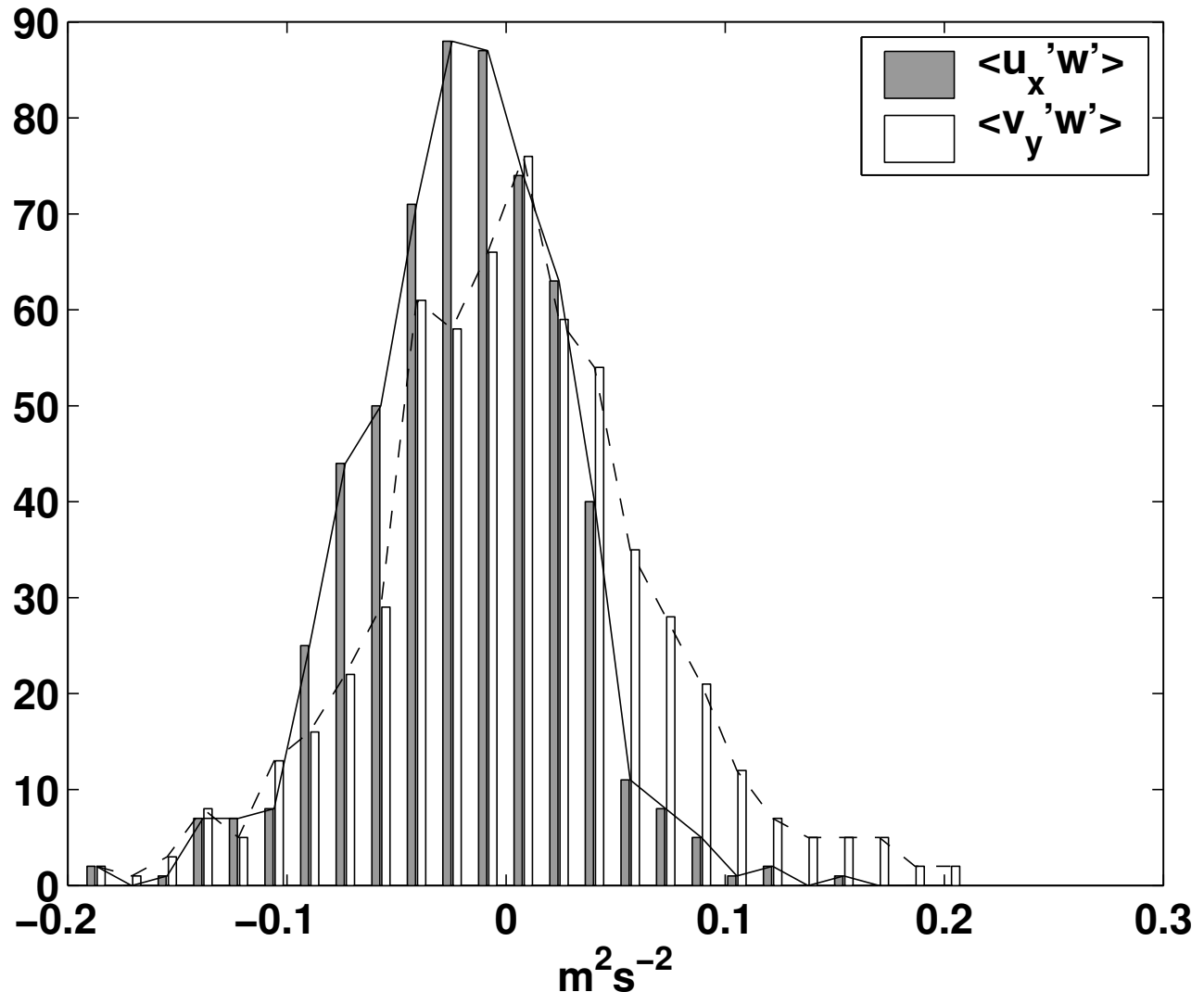


Figure 8: Distributions of the longitudinal (top) and transverse (bottom) components of the momentum flux. All legs and all flights are included. New dataset.

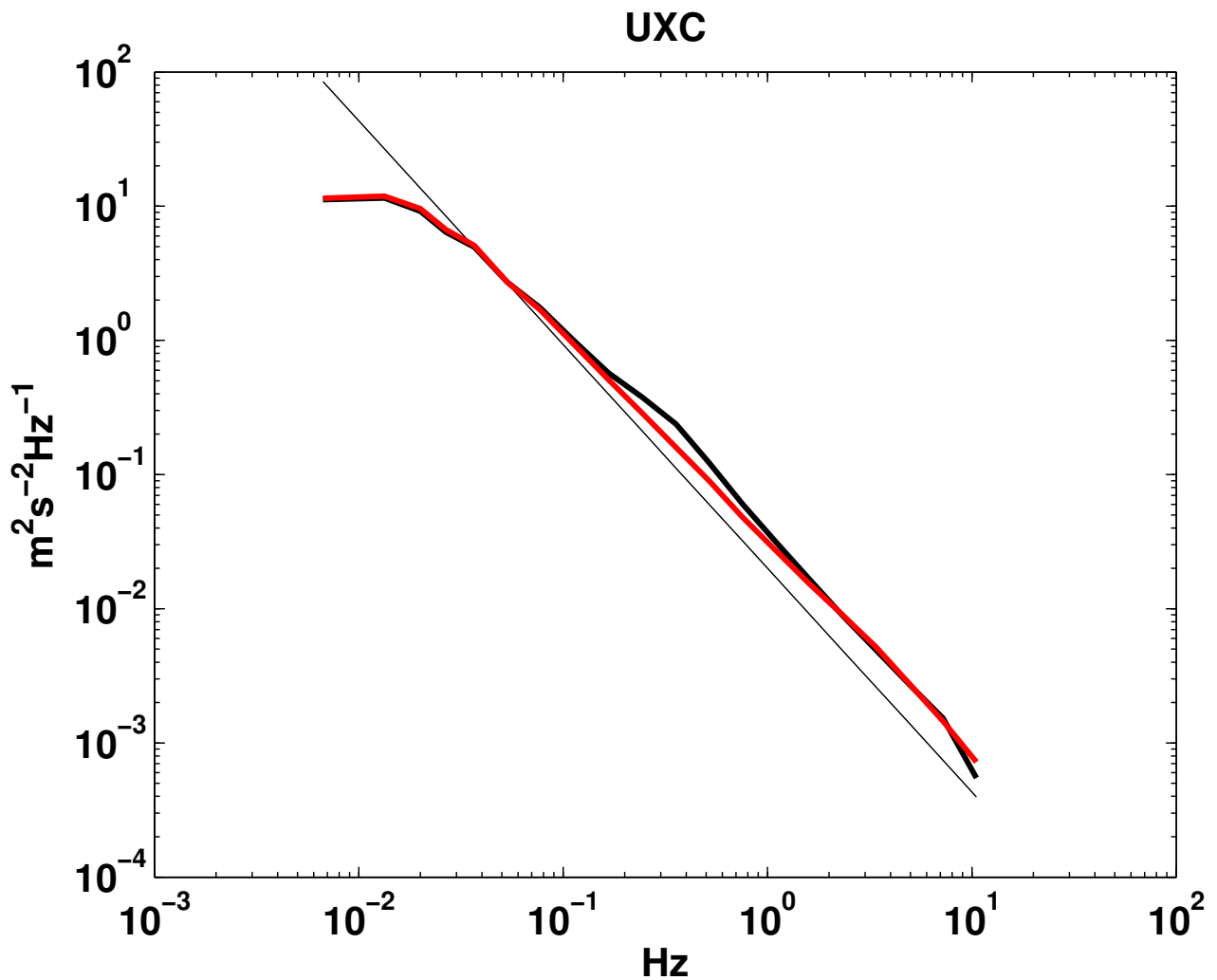


Figure 9: Mean spectrum of the longitudinal wind component over all legs and flights, for the two different datasets. Red is the new dataset and black is the original dataset.

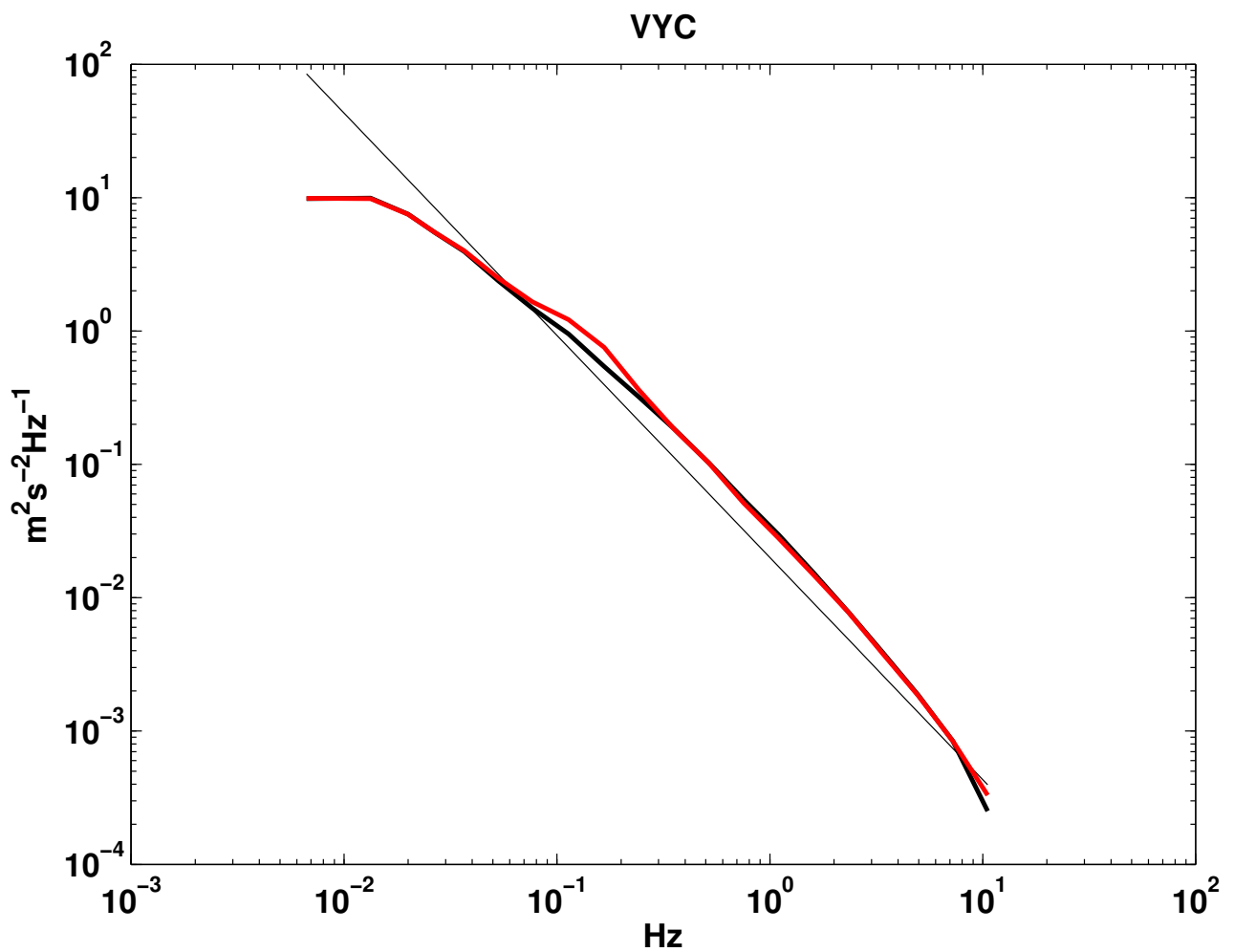


Figure 10: Mean spectrum of the lateral wind component over all legs and flights, for the two different datasets. Red is the new dataset and black is the original dataset.

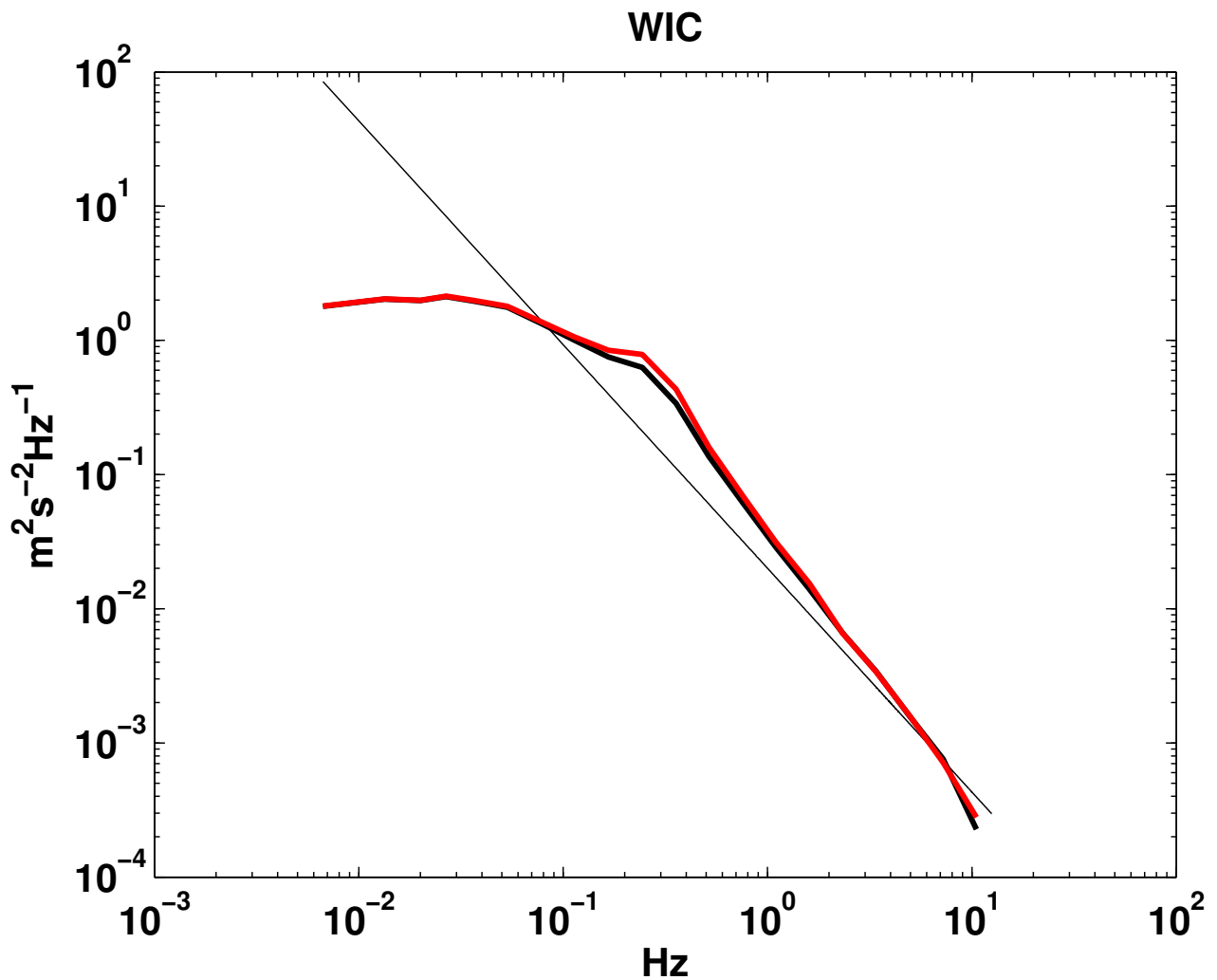


Figure 11: Mean spectrum of the vertical wind component over all legs and flights, for the two different datasets. Red is the new dataset and black is the original dataset.

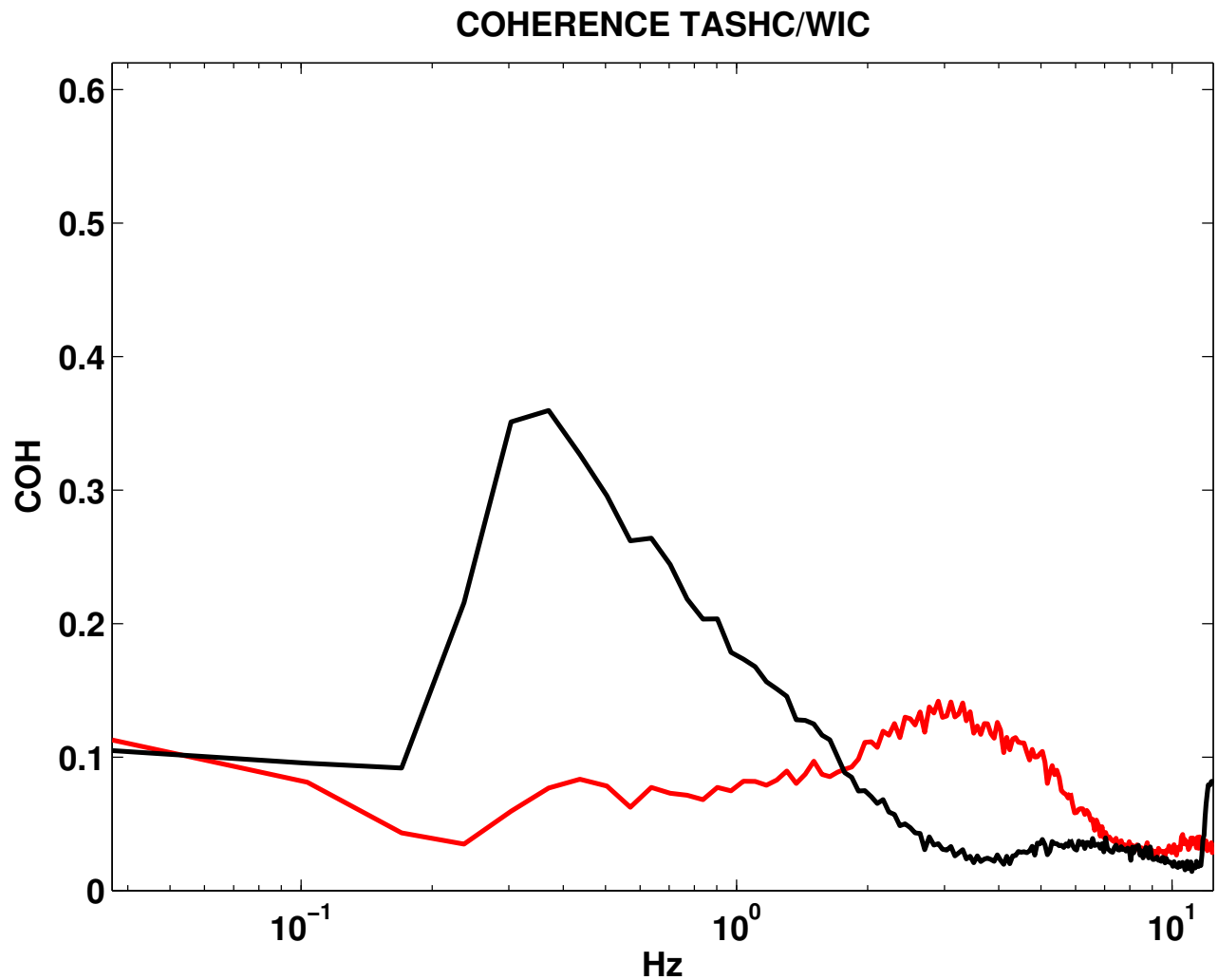


Figure 12: Mean coherence between the true air speed and the vertical velocity during all flights all legs, for the two different datasets. Red is the new dataset and black is the original dataset.